SIAM J. IMAGING SCIENCES
Vol. 3, No. 3, pp. 416–433

Higher Order Positive Semidefinite Diffusion Tensor Imaging*

Liqun Qi†, Gaohang Yu‡, and Ed X. Wu§

Abstract. Due to the well-known limitations of diffusion tensor imaging, high angular resolution diffusion imaging (HARDI) is used to characterize non-Gaussian diffusion processes. One approach to analyzing HARDI data is to model the apparent diffusion coefficient (ADC) with higher order diffusion tensors. The diffusivity function is positive semidefinite. In the literature, some methods have been proposed to preserve positive semidefiniteness of second order and fourth order diffusion tensors. None of them can work for arbitrarily high order diffusion tensors. In this paper, we propose a comprehensive model to approximate the ADC profile by a positive semidefinite diffusion tensor of either second or higher order. We call this the positive semidefinite diffusion tensor (PSDT) model. PSDT is a convex optimization problem with a convex quadratic objective function constrained by the nonnegativity requirement on the smallest Z-eigenvalue of the diffusivity function. The smallest Z-eigenvalue is a computable measure of the extent of positive definiteness of the diffusivity function. We also propose some other invariants for the ADC profile analysis. Experiment results show that higher order tensors could improve the estimation of anisotropic diffusion and that the PSDT model can depict the characterization of diffusion anisotropy which is consistent with known neuroanatomy.

Key words. positive semidefinite diffusion tensor, apparent diffusion coefficient, Z-eigenvalue, convex optimization problem, invariants

AMS subject classifications. 58J65, 65H17, 65K05

DOI. 10.1137/090755138

1. Introduction.

The diffusion tensor imaging (DTI) model was proposed in 1994 by Basser, Mattiello, and LeBihan [6, 7], and is now widely used in biological and clinical research [5]. However, DTI is known to have a limited capability in resolving multiple fiber orientations within one voxel. This is mainly because the probability density function for random spin displacement is non-Gaussian in complex fiber configuration, such as when fiber bundles cross or diverge within the same voxel. Thus, the modeling of self-diffusion by a second order tensor breaks down in such cases.

In order to describe the non-Gaussian diffusion process, high angular resolution diffusion imaging (HARDI) has been proposed by Tuch et al. [34]. The idea of HARDI is to sample

*Received by the editors April 6, 2009; accepted for publication (in revised form) June 2, 2010; published electronically August 19, 2010. This work was partly supported by the Research Grant Council of Hong Kong, a postdoctoral fellowship from the Department of Applied Mathematics at the Hong Kong Polytechnic University, a grant from the Ph.D. Programs Foundation of Ministry of Education of China (200805581022), and the National Natural Science Foundation of China (10926029).

http://www.siam.org/journals/siims/3-3/75513.html

†Department of Applied Mathematics, The Hong Kong Polytechnic University, Hung Hom, Kowloon, Hong Kong (maqilq@polyu.edu.hk).

‡Jiangxi Key Laboratory of Numerical Simulation Technology, School of Mathematics and Computer Sciences, GanNan Normal University, Ganzhou, 341000, China (maghyu@163.com). Current address: Department of Applied Mathematics, The Hong Kong Polytechnic University, Hung Hom, Kowloon, Hong Kong.

§Department of Electrical and Electronic Engineering, The University of Hong Kong, Hong Kong (ewu@eee.hku.hk).

the sphere in N discrete gradient directions and compute the apparent diffusion coefficient (ADC) profile along each direction, without an a priori assumption about the nature of the diffusion process within the voxel. A number of approaches have been put forth to analyze HARDI data [1, 11, 12, 14, 19, 33]. One natural generalization is to model the ADC profile with higher order diffusion tensors (HODT) [23]. This model does not assume any a priori knowledge about the diffusivity profile and has the potential to describe the non-Gaussian diffusion. Also, there are some other models, such as the continuous mixture of Gaussian models [18], which could also deal with complex local geometries.

An intrinsic property of the diffusivity profile is positive semidefiniteness [3, 4, 9, 15, 35]. Hence, the diffusion tensor, either second or higher order, must be positive semidefinite. For the second order diffusion tensor, one may diagonalize it and project it to the symmetric positive semidefinite cone by setting the negative eigenvalues to zero [11]. Recently, the authors in [4] proposed a ternary quartics approach to preserve positive semidefiniteness for a fourth order diffusion tensor. In [15], by mapping a fourth order three-dimensional tensor to a second order six-dimensional tensor which is a 6×6 matrix, the authors extended the Riemannian framework from second order tensors [2, 20, 25] to the space of fourth order tensors. Furthermore, they proceeded to use the Riemannian framework for S^+ in the space $S^+(6)$ to guarantee a positive diffusion function. However, none of them is comprehensive enough to work for arbitrarily high order diffusion tensors.

In the next section, we propose approximating the ADC profile by a positive semidefinite diffusion tensor of either second or higher order. We show that this model is a convex optimization problem with a convex quadratic objective function. In a certain sense, this model is the least squares problem under the positive semidefiniteness constraint. Under a full rank assumption on the sample gradient directions, we show that this model has a unique global minimizer. If the least squares solution is in the positive semidefinite region, then it is the global minimizer of this model. Otherwise, we show that the global minimizer of this model is on the boundary of the positive semidefiniteness region.

The constraint of the model discussed in section 2 is not explicit. On the other hand, the smallest Z-eigenvalue of the diffusivity function is a computable measure for the extent of positive definiteness of the diffusivity function. In the appendix (section 7), we explain the definition of the smallest Z-eigenvalue and present a computational method for calculating it.

In section 3 we propose a comprehensive model for approximating the ADC profile. We call this the positive semidefinite diffusion tensor (PSDT) model. In essence, PSDT is the model in section 2, with an explicit constraint; i.e., the smallest Z-eigenvalue of the diffusivity function is nonnegative. We show that the smallest Z-eigenvalue is a concave function of the diffusivity function. We also give an optimality condition for PSDT and the expression of the subdifferential of the smallest Z-eigenvalue function.

In the DTI model, there are several characteristic quantities for the ADC profile. These include the three eigenvalues of the second order diffusion tensor, the mean diffusivity, and the fractional anisotropy. In [24], Özarslan, Vemuri, and Mareci proposed some rotationally invariant parameters for HODT. In section 4, we propose several characteristic quantities for PSDT.

Performance of PSDT is depicted in section 5 on synthetic data as well as on MRI data. Experiment results show that higher order tensors could improve the estimation of anisotropic

diffusion and that the PSDT model can depict the characterization of diffusion anisotropy which is consistent with known neuroanatomy. Section 6 is the conclusion.

2. Positive semidefinite diffusion tensor. We use $\mathbf{g} = (g_1, g_2, g_3)^T$ to denote the magnetic field gradient direction [4]. Assume that we use an mth order diffusion tensor. Then the diffusivity function can be expressed as

$$d(\mathbf{g}) = \sum_{i=0}^{m} \sum_{j=0}^{m-i} d_{ij} g_1^i g_2^j g_3^{m-i-j}. \tag{2.1}$$

A diffusivity function d can be regarded as an mth order symmetric tensor [8, 11, 12, 23, 26]. Clearly, there are

$$n = \sum_{i=1}^{m+1} i = \frac{1}{2}(m+1)(m+2)$$

terms [23, 11] in (2.1). Hence, each diffusivity function can also be regarded as a vector in $\Re^n$.

We may think that any vector in $\Re^n$ is indexed by ij, where $j = 0, \ldots, m-i, i = 0, \ldots, m$. In this way, we may regard $\hat{g}$ as a vector in $\Re^n$, whose ijth component is $g_1^i g_2^j g_3^{m-i-j}$. Then we may rewrite (2.1) as

$$d(\mathbf{g}) = d^\top \hat{g};$$

i.e., we may regard $d(\mathbf{g})$ as the scalar product of vectors d and $\hat{g}$. This point of view will be useful later.

We say that d is positive semidefinite if for all $\mathbf{g} \in \Re^3$, $d(\mathbf{g}) \geq 0$. Since we may regard d as a vector in $\Re^n$, we say that d is a positive semidefinite vector in $\Re^n$ in this case. Clearly, m should be even such that there are nonzero positive semidefinite vectors. Denote the set of all positive semidefinite vectors as $\mathcal{S}_m$, or simply $\mathcal{S}$ when m is fixed.

Theorem 2.1. *$\mathcal{S}$ is a closed convex cone in $\Re^n$.*

Proof. Let $d^{(1)}, d^{(2)} \in \mathcal{S}$ and $a, b \geq 0$. Let $d = ad^{(1)} + bd^{(2)}$. For any $\mathbf{g} \in \Re^3$,

$$d(\mathbf{g}) = \sum_{i=0}^{m} \sum_{j=0}^{m-i} d_{ij} g_1^i g_2^j g_3^{m-i-j} = \sum_{i=0}^{m} \sum_{j=0}^{m-i} \left(a d_{ij}^{(1)} + b d_{ij}^{(2)} \right) g_1^i g_2^j g_3^{m-i-j}$$

$$= a d^{(1)}(\mathbf{g}) + b d^{(2)}(\mathbf{g}) \geq 0.$$

Hence $d \in \mathcal{S}$. This proves that $\mathcal{S}$ is a convex cone. Let $\{d^{(k)}\} \subset \mathcal{S}$ and $\lim_{k\to\infty} d^{(k)} = d$. For any $\mathbf{g} \in \Re^3$,

$$d(\mathbf{g}) = \lim_{k\to\infty} d^{(k)}(\mathbf{g}) \geq 0.$$

This shows that $\mathcal{S}$ is closed. The proof is complete. ∎

Suppose that we sample the ADC values in N gradient directions $\{g^{(l)} : l = 1, \ldots, N\}$, $N \geq n$, and that the corresponding ADC values on these N gradients are $\{b_l : l = 1, \ldots, N\}$. Then $\{\hat{g}^{(l)} : l = 1, \ldots, N\}$ are N vectors in $\Re^n$. We assume that $\{\hat{g}^{(l)} : l = 1, \ldots, N\}$ spans $\Re^n$, i.e., there are n vectors among these N vectors which are linearly independent, or we say that $\{\hat{g}^{(l)} : l = 1, \ldots, N\}$ has rank n. We call this assumption the *full rank assumption*. This

assumption is necessary so that the N gradient directions $\{g^{(l)} : l = 1, \ldots, N\}$ can reflect the ADC profile sufficiently. When N is relatively big, this assumption would be satisfied in general. Let A be an $n \times N$ matrix whose column vectors are $\hat{g}^{(l)}, l = 1, \ldots, N$. Let $B = AA^\top$. Then B is an $n \times n$ positive semidefinite symmetric matrix. Under the full rank assumption, B is a positive definite symmetric matrix. We also let b be a vector in $\Re^N$, with components $\{b_l : l = 1, \ldots, N\}$.

The least squares problem for finding a diffusivity function to reflect the ADC profile is to find $\bar{d} \in \Re^n$ such that

$$L(\bar{d}) = \min_{d \in \Re^n} L(d), \tag{2.2}$$

where

$$L(d) = \sum_{l=1}^{N} \left(d(\mathbf{g}^{(l)}) - b_l\right)^2 = \sum_{l=1}^{N} \left(\left(\hat{g}^{(l)}\right)^\top d - b_l\right)^2.$$

It is well known that under the full rank assumption the solution of the least squares problem (2.2) is

$$\bar{d} = B^{-1}Ab. \tag{2.3}$$

As $\bar{d}$ may not be positive semidefinite, we formulate a new model as

$$L(d^*) = \min_{d \in \mathcal{S}} L(d). \tag{2.4}$$

In a certain sense, (2.4) is the least squares problem under the positive semidefiniteness constraint.

The function L is a convex quadratic function. Actually, by (2.3), for any $d \in \Re^n$, we have

$$L(d) = (d - \bar{d})^\top B(d - \bar{d}). \tag{2.5}$$

The constraint of (2.4) is not in an explicit function form. However, we may use PSDT to get some important theoretical properties of the solution. In particular, we will show that if $\bar{d} \notin \mathcal{S}$, then d^* is on the boundary of $\mathcal{S}$. This property is useful for calculating d^* in this case. We now have the following theorem.

Theorem 2.2. *Problem* (2.4) *is a convex optimization problem with a convex quadratic objective function. If* $\bar{d} \in \mathcal{S}$, *then* $d^* = \bar{d}$ *is a global minimizer of* (2.4).

Furthermore, assume that the full rank assumption holds. Then (2.4) *has a unique solution* d^*. *In this case, if* $\bar{d} \notin \mathcal{S}$, *then* d^* *is on* $\partial\mathcal{S}$, *the boundary of* $\mathcal{S}$.

Proof. The first two conclusions follow directly from Theorem 2.1, (2.4), and (2.5).

We now assume that the full rank assumption holds. Clearly, $d = 0$ is in $\mathcal{S}$, and hence is a feasible solution of (2.4). Therefore, we may add an additional constraint

$$L(d) \le L(0),$$

i.e.,

$$(d - \bar{d})^\top B(d - \bar{d}) \le \bar{d}^\top B\bar{d},$$

to (2.4). As the full rank assumption holds, B is positive definite. Then, the additional constraint makes the feasible region compact. Thus, (2.4) has a global minimizer d^* in this case. According to convex analysis [31], the optimality condition of (2.4) is

$$-\nabla L(d^*) \in N_{\mathcal{S}}(d^*), \tag{2.6}$$

where $N_{\mathcal{S}}(d^*)$ is the normal cone of $\mathcal{S}$ at d^*. By (2.5), $\nabla L(d^*) = 2B(d^* - \bar{d})$. By the definition of the normal cone [31], (2.6) implies that for any $d \in \mathcal{S}$, we have

$$(\bar{d} - d^*)^\top B(d - d^*) \le 0.$$

Suppose that d^{**} is also a global minimizer of (2.4). Then the above inequality implies that

$$(\bar{d} - d^*)^\top B(d^{**} - d^*) \le 0$$

and

$$(\bar{d} - d^{**})^\top B(d^* - d^{**}) \le 0.$$

Summing up these two inequalities, we have

$$(d^{**} - d^*)^\top B(d^{**} - d^*) \le 0.$$

Since B is positive definite, this implies that $d^{**} = d^*$; i.e., d^* is the unique global minimizer of (2.4).

Under the full rank assumption, if $\bar{d} \notin \mathcal{S}$, then $d^* \neq \bar{d}$ as $d^* \in \mathcal{S}$. Consider the segment

$$[d^*, \bar{d}] \equiv \{d^* + t(\bar{d} - d^*) : 0 \le t \le 1\}.$$

As $\mathcal{S}$ is a closed convex set, $\bar{d} \notin \mathcal{S}$, and $d^* \in \mathcal{S}$, there is $t_0 \in [0, 1)$ such that $d^* + t_0(\bar{d} - d^*)$ is on $\partial\mathcal{S}$, the boundary of $\mathcal{S}$. As d^* is the unique global minimizer of (2.4), we have

$$L(d^*) \le L(d^* + t_0(\bar{d} - d^*)),$$

i.e.,

$$(d^* - \bar{d})^\top B(d^* - \bar{d}) \le \left(d^* + t_0(\bar{d} - d^*) - \bar{d}\right)^\top B\left(d^* + t_0(\bar{d} - d^*) - \bar{d}\right)$$

$$= (1 - t_0)^2 (d^* - \bar{d})^\top B(d^* - \bar{d}).$$

As $(d^* - \bar{d})^\top B(d^* - \bar{d}) > 0$, this implies that $t_0 = 0$; i.e., d^* is on $\partial\mathcal{S}$, the boundary of $\mathcal{S}$. This completes the proof. ∎

How, then, to identify $\bar{d} \in \mathcal{S}$? In the appendix, we will show that $d \in \mathcal{S}$ if and only if $\lambda_{\min}(d)$, the smallest Z-eigenvalue of d, is nonnegative. We will also provide a computational method for calculating $\lambda_{\min}(d)$.

3. The PSDT model. With the discussion in section 2, we are in a position to formulate an explicit constraint for (2.4). We call this the PSDT (positive semidefinite diffusion tensor) model. It is as follows:

$$L(d^*) = \min\{L(d) : \lambda_{\min}(d) \geq 0\}. \tag{3.1}$$

The function value of $\lambda_{\min}(d)$ is computable with the method provided in the appendix.

Theorem 3.1. *$\lambda_{\min}(d)$ is a continuous concave function. Hence, PSDT (3.1) is a convex optimization problem.*

Furthermore, suppose that the full rank assumption holds and $\bar{d} \notin \mathcal{S}$. Then d^* is the unique global minimizer of PSDT (3.1) if and only if there is a positive number μ such that

$$\begin{cases} B(d^* - \bar{d}) &= \mu \hat{g}^*, \\ \lambda_{\min}(d^*) &= 0, \end{cases} \tag{3.2}$$

where $\hat{g}^*$ is a subgradient [31] of the concave function $\lambda_{\min}$ at d^*. By (3.2), we have

$$\begin{cases} (d^*)^\top B(d^* - \bar{d}) &= 0, \\ (\hat{g}^*)^\top d^* &= 0. \end{cases} \tag{3.3}$$

Proof. Let $d^{(1)}, d^{(2)} \in \Re^n$, $0 \leq t \leq 1$, and $d = td^{(1)} + (1-t)d^{(2)}$. Suppose $\mathbf{g}^*$ is a global minimizer of (7.1). Then $(g_1^*)^2 + (g_2^*)^2 + (g_3^*)^2 = 1$, and

$$\lambda_{\min}(d) = d(\mathbf{g}^*) = td^{(1)}(\mathbf{g}^*) + (1-t)d^{(2)}(\mathbf{g}^*) \geq t\lambda_{\min}(d^{(1)}) + (1-t)\lambda_{\min}(d^{(2)}).$$

This shows that $\lambda_{\min}(d)$ is a concave function. Since $\lambda_{\min}$ is a concave function defined in the whole space $\Re^n$, according to convex analysis [31], it is a continuous function. Since L is a convex quadratic function, PSDT is also a convex optimization problem.

Furthermore, suppose that the full rank assumption holds and $\bar{d} \notin \mathcal{S}$. By Theorem 2.2 and (2.4), PSDT (3.1) has a unique global minimizer d^*, and d^* is on the boundary of $\mathcal{S}$. Since $\lambda_{\min}(d)$ is continuous, we have $\lambda_{\min}(d^*) = 0$. Since $\bar{d} \notin \mathcal{S}$, we know that $d^* \neq \bar{d}$ and $\nabla L(d^*) \neq 0$. Now, (3.2) follows from (2.5) and the optimality condition of the convex optimization problem PSDT (3.1). By (7.3), we have

$$\lambda_{\min}(d^*) = (\hat{g}^*)^\top d^*.$$

From this and the second equation of (3.2), we have the second equation of (3.3). Let the two sides of the first equation of (3.2) take inner product with d^*. Combining this with the second equation of (3.3), we have the first equation of (3.3). ∎

Suppose that $\mathbf{g}$ is a global minimizer of (7.1). By (7.3), we have

$$\lambda_{\min}(d) = \hat{g}^\top d. \tag{3.4}$$

When m is even, if $\mathbf{g}$ is a global minimizer of (7.1), then $\mathbf{h} = -\mathbf{g}$ is also a global minimizer of (7.1). However, we have $\hat{g} = \hat{h}$ in this case. Therefore, such a $\hat{g}$ in (3.4), generated by a global minimizer $\mathbf{g}$, may still be unique even if the global minimizers are not unique. By convex analysis, we know that if such a $\hat{g}$ in (3.4) is unique, then $\lambda_{\min}(d)$ is differentiable at

d and its gradient is $\hat{g}$. If such a $\hat{g}$ is not unique, then any such $\hat{g}$ is a subgradient of $\lambda_{\min}(d)$ at d and the subdifferential of $\lambda_{\min}(d)$ at d is the convex hull of all such $\hat{g}$'s.

Based on these, we may solve PSDT (3.1) by a standard convex programming method [17]. Under the full rank assumption, we may use (2.3) to calculate $\bar{d}$. If $\lambda_{\min}(\bar{d}) \geq 0$, then $d^* = \bar{d}$ and the task is completed. If $\lambda_{\min}(\bar{d}) < 0$, by Theorem 3.1, $\lambda_{\min}(d^*) = 0$. Hence, in this case, we need only solve the model

$$L(d^*) = \min\{L(d) : \lambda_{\min}(d) = 0\}, \tag{3.5}$$

which has only an equality constraint. However, it is not a convex optimization problem. On the other hand, (3.2) is still its optimality condition. If we use the subgradient of $\lambda_{\min}(d)$ as a substitute for its gradient, according to numerical optimization [22], we may use a gradient descent method to solve (3.5).

We may also apply the analytical center cutting plane method in [16] to solve the nondifferentiable convex optimization problem (3.1). Then problem (3.1) is theoretically polynomial-time solvable by [16]. In section 5, where the gradient descent method is used, we may also see that this problem is practically solvable.

4. Characteristic quantities of PSDT. In the DTI model, there are some characteristic quantities which play important roles in the ADC profile analysis of DTI. These characteristic quantities are rotationally invariant, independent from the choice of the laboratory coordinate system. They include the three eigenvalues $\lambda_1 \geq \lambda_2 \geq \lambda_3$ of the second order diffusion tensor D, the mean diffusivity (M_D), and the fractional anisotropy (FA). The largest eigenvalue λ_1 describes the diffusion coefficient in the direction parallel to the fibers in the human tissue. The other two eigenvalues describe the diffusion coefficient in the direction perpendicular to the fibers in the human tissue. The mean diffusivity is

$$M_D = \frac{\lambda_1 + \lambda_2 + \lambda_3}{3},$$

while the FA is

$$FA = \sqrt{\frac{3}{2}}\sqrt{\frac{(\lambda_1 - M_D)^2 + (\lambda_2 - M_D)^2 + (\lambda_3 - M_D)^2}{\lambda_1^2 + \lambda_2^2 + \lambda_3^2}},$$

where $0 \leq FA \leq 1$. If $FA = 0$, the diffusion is isotropic. If $FA = 1$, the diffusion is anisotropic.

In [24], Özarslan, Vemuri, and Mareci generalized the well-known FA measure for HARDI data fitting with higher order tensors. They proposed a generalized anisotropy (GA) measure which is based on the generalization of the trace and the variance of the normalized diffusivity $d_N(g) \triangleq \frac{d(g)}{\text{gentr}(d(g))}$. Let the unit hemisphere be denoted by Ω; then the generalized trace $\text{gentr}(d(g))$ is defined as

$$\text{gentr}(d(g)) = \frac{3}{2\pi}\int_{\Omega} d(g)dg.$$

The generalized variance of normalized diffusivity is given by

$$V = \frac{1}{3}\left(\text{gentr}(d_N(g)^2) - \frac{1}{3}\right).$$

And the final GA measure is defined as

$$GA = 1 - \frac{1}{1 + (250V)^{\varepsilon(V)}}, \quad \text{where } \varepsilon(V) = 1 + \frac{1}{1 + 5000V}.$$

Just as FA in the DTI case, GA also possesses the property of being scaled between 0 and 1. Furthermore, GA does not assume any specified approximation order.

According to [26, 27], the Z-eigenvalues are also rotationally invariant. Hence, we may use them and their functions as characteristic quantities of PSDT. In [8], Z-eigenvalues have already been proposed for HODT.

After finding the global minimizer d^* of PSDT, we may use the method in the appendix to calculate $\lambda_{\min} = \lambda_{\min}(d^*)$ and the other Z-eigenvalues of d^* as $\lambda_1 \geq \lambda_2 \geq \cdots \geq \lambda_\nu \geq 0$. Then $\lambda_1 = \lambda_{\max}$ and $\lambda_\nu = \lambda_{\min}$. By [21], we may conclude that in the regular case, the number ν of Z-eigenvalues of d^* satisfies $\nu \leq m^2 - m + 1$.

As we discussed before, $\lambda_{\min}$ is a measure of the extent of positive definiteness of d^*. On the other hand, if $(\mathbf{g}^{\max}, \lambda_{\max})$ is a solution of (7.2), then $\mathbf{g}^{\max}$ is the principal ADC direction, as discussed in [8]. Along this principal direction $\mathbf{g}^{\max}$, the ADC value of d^* attains its maximum.

We define the PSDT mean value as

$$M_{PSDT} = \frac{1}{\nu} \sum_{i=1}^{\nu} \lambda_i,$$

and define the PSDT fractional anisotropy similarly to [32, 30] as

$$FA_{PSDT} = \sqrt{\frac{\nu}{\nu - 1}} \sqrt{\frac{\sum_{i=1}^{\nu} (\lambda_i - M_{PSDT})^2}{\sum_{i=1}^{\nu} \lambda_i^2}}.$$

Then we have $0 \leq FA_{PSDT} \leq 1$. If $FA_{PSDT} = 0$, the diffusion is isotropic. If $FA_{PSDT} = 1$, the diffusion is anisotropic.

5. Numerical examples. Here we present some numerical examples to explain our experiments and their motivations. First, we report some computational results of the synthetic data experiment. We generated the synthetic diffusion weighted images using the following multitensor model [1]:

$$S(g_i) = \sum_{k=1}^{f} p_k e^{-b g_i D_k g_i} + \text{noise}, \tag{5.1}$$

where $f \in \{0, 1, 2, 3\}$ is the number of fibers, p_k is the proportion of tissue in the voxel that corresponds to the kth fiber ($\sum_{k=1}^{f} p_k = 1$), b is the b-value, g_i is the ith gradient direction for $i \in \{1, \ldots, 81\}$, and D_k is the diffusion tensor of the kth fiber. The noise was typically generated by Rician noise (complex Gaussian noise) with standard deviation of $1/\sigma$, producing a signal to noise ratio (SNR) of σ. In our experiments, the b-value is equal to 3000 sec/mm^2 and the diffusion tensors were selected, such as $D_k = \text{diag}(1700, 100, 100) \times 10^{-6}$ mm^2/sec

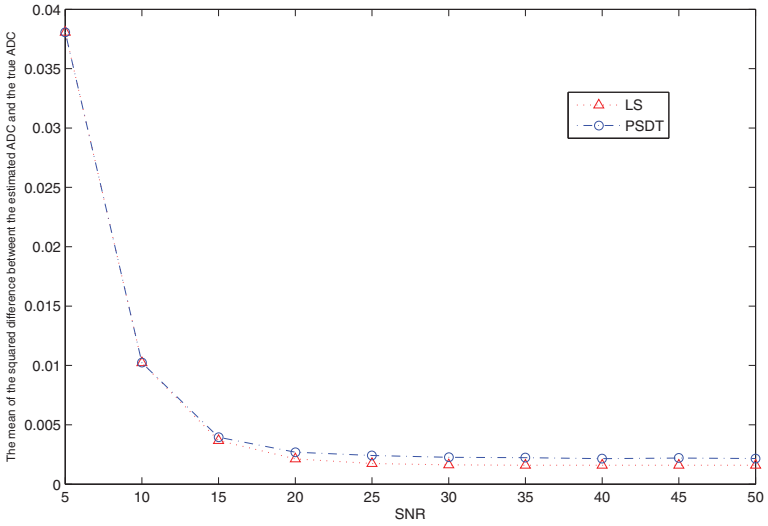

Figure 1. *Comparison of our method with the least squares (LS) method for a one-fiber test, fitting with a fourth order tensor.*

for $k = 1, 2, 3$. We generated Rician-corrupted data S as done in [13, 36]. For each noise-free data x, we computed S as

$$S = \sqrt{\left(\frac{x}{\sqrt{2}} + n_r\right)^2 + \left(\frac{x}{\sqrt{2}} + n_i\right)^2},$$

where n_r and $n_i \sim \mathcal{N}(0, \sigma^2)$. The value S is the realization of a random variable with a Rician probability density function of parameters x and σ.

In order to compare the robustness of our method in the presence of noise, we generated the signals by (5.1) at 10 different SNRs ranging from 5 to 50 and repeated the experiments 10 times. Then, as done in [11], we computed the mean of the pointwise squared difference between the estimated ADC points and points on the ground truth ADC profiles (noise-free in (5.1)); i.e., $E_i = (S(g_i) - S_{true}(g_i))^2$. The results are plotted in Figures 1 and 2, which correspond to ADC functions fitting with a fourth order diffusion tensor and a sixth order tensor, respectively. The CPU time of Z-eigenvalue calculation at each iteration is about 0.06 *sec* when the ADC function is fitted with a fourth order tensor, or 0.2 *sec* when it is fitted with a sixth order tensor. As would be expected, the mean of the squared errors decreases as the SNR increases. The PSDT method compares favorably to the LS method. As can be seen from Figures 1 and 2, the mean of the squared errors will also decrease when the ADC function is fitted with a higher order tensor. In Figure 1, when the SNR is greater than 15, the mean squared errors generated by the PSDT method are below 0.0026 and the errors generated by the LS method are about 0.0018. In Figure 2, the PSDT method and the LS method generated a similar mean squared error. We can see from Figure 2 that even at a low SNR of 10, the mean squared error generated by the PSDT method is about 0.01, while at an SNR of 25 it drops to 0.0007.

The LS method is a simple approach to estimating the coefficients of an ADC function,

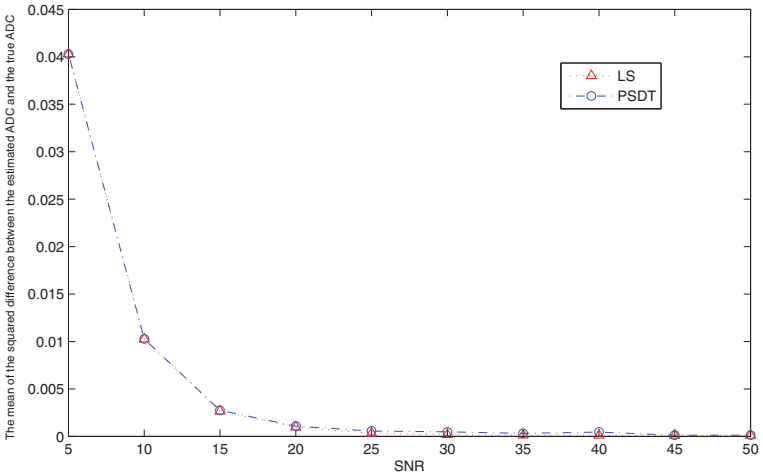

Figure 2. *Comparison of our method with the LS method for a one-fiber test, fitting with a sixth order tensor.*

Table 1
Z-eigenvalues and eigenvectors of ADC_{LS}.

	g_1	g_2	g_3	λ
1	-0.0114	-0.9312	0.3644	0.6774
2	0.828	0.4958	0.2619	-0.0297
3	-0.0091	0.8683	0.4959	0.6988
4	-0.844	-0.4156	0.3389	-0.0178
5	-0.8376	0.2439	0.4888	-0.0349
6	-0.0112	-0.5166	0.8561	0.6854
7	0.8313	-0.1746	0.5276	-0.0087
8	-0.0063	0.1465	0.9892	0.6761
9	0.9997	-0.0012	0.0234	0.112

which is fast but does not guarantee positive diffusivity. For example, in the single tensor model, the ADC function (without noise) estimated by the LS method, fitting with a fourth order tensor, is $ADC(g) = d_{LS}^T \hat{g}$, where d_{LS} is a vector of dimension 15 with $d_{LS}(1) = 0.1115$, $d_{LS}(2) = 0.6848$, $d_{LS}(3) = 0.6771$, $d_{LS}(4) = -0.0005$, $d_{LS}(5) = 0.0408$, $d_{LS}(6) = 0.0096$, $d_{LS}(7) = 0.0363$, $d_{LS}(8) = -0.0245$, $d_{LS}(9) = -0.0142$, $d_{LS}(10) = -0.68$, $d_{LS}(11) = -0.6507$, $d_{LS}(12) = 1.3911$, $d_{LS}(13) = -0.0739$, $d_{LS}(14) = -0.114$, $d_{LS}(15) = 0.0049$. In our experiment, $\hat{g}$ is ordered as $\hat{g}(1) = g_1^4$, $\hat{g}(2) = g_2^4$, $\hat{g}(3) = g_3^4$, $\hat{g}(4) = g_1^3 g_2$, $\hat{g}(5) = g_1^3 g_3$, $\hat{g}(6) = g_1 g_2^3$, $\hat{g}(7) = g_2^3 g_3$, $\hat{g}(8) = g_1 g_3^3$, $\hat{g}(9) = g_2 g_3^3$, $\hat{g}(10) = g_1^2 g_2^2$, $\hat{g}(11) = g_1^2 g_3^2$, $\hat{g}(12) = g_2^2 g_3^2$, $\hat{g}(13) = g_1^2 g_2 g_3$, $\hat{g}(14) = g_1 g_2^2 g_3$, $\hat{g}(15) = g_1 g_2 g_3^2$. Using the method provided in the appendix, we can compute all the Z-eigenvalues and the associated eigenvectors, which are listed in Table 1. From Table 1, we can see that there are four negative eigenvalues and the smallest Z-eigenvalue is -0.0349, attained at $(-0.8376, 0.2439, 0.4888)$.

But the PSDT method can guarantee positive diffusivity. In the same case, the ADC function estimated by the PSDT method is $ADC(g) = d_{PSDT}^T \hat{g}$, with $d_{PSDT}(1) = 0.1287$, $d_{PSDT}(2) = 0.7023$, $d_{PSDT}(3) = 0.6931$, $d_{PSDT}(4) = 0.0$, $d_{PSDT}(5) = 0.0409$, $d_{PSDT}(6) = 0.0101$, $d_{PSDT}(7) = 0.0363$, $d_{PSDT}(8) = -0.0246$, $d_{PSDT}(9) = -0.014$, $d_{PSDT}(10) = -0.5627$,

Table 2
Z-eigenvalues and eigenvectors of ADC_{PSDT}.

	g_1	g_2	g_3	λ
1	-0.0070	-0.9877	0.1560	0.6995
2	0.8369	0.5072	0.2056	0.0065
3	-0.0104	0.7920	0.6105	0.7340
4	-0.8539	-0.4006	0.3322	0.0178
5	-0.0134	-0.6540	0.7564	0.7213
6	0.8399	-0.2026	0.5035	0.0267
7	-0.8454	0.1949	0.4974	0.0003
8	-0.0064	0.0556	0.9984	0.6928
9	0.9997	-0.0012	0.0259	0.1292

$d_{PSDT}(11) = -0.5331$, $d_{PSDT}(12) = 1.5083$, $d_{PSDT}(13) = -0.0739$, $d_{PSDT}(14) = -0.1141$, $d_{PSDT}(15) = 0.0049$. We compute all Z-eigenvalues and the associated eigenvectors, and list them in Table 2. We can see that the smallest Z-eigenvalue is 0.0003, attained at $(-0.8454, 0.1949, 0.4974)$.

In the next experiment, we are interested in estimating the ADC profiles from a human brain dataset with a size of $90 \times 90 \times 60$, which was acquired on a 1.5T scanner at $b = 1000$ sec/mm^2 using 60 encoding directions, with voxel dimensions of 1.875 $mm \times 1.875$ $mm \times 2$ mm. In this experiment we first visualized some characteristic quantities of the PSDT model by MATLAB 7.4, fitting with a fourth order tensor. In Figure 3, we show all the coefficients of the ADC profile d in the row order. As observed in [23], the coefficients of even degrees (such as c_{iiii} or c_{iijj}, $i, j = 1, 2, 3$) are greater than the other coefficients. Figure 4 shows the map of M_{PSDT} in which the values are scaled to $[0, 1]$.

Finally, for comparison, we also estimated the GA and FA_{PSDT} at each voxel fitting with second, fourth, and sixth order tensors, respectively. We found that no negative eigenvalue happens in our experiments. So, there is no practical difference observed between the LS method and the PSDT method. When the ADC function is fitted with a second order tensor, the Z-eigenvalues will reduce to the traditional eigenvalues of a matrix. So, in this case, the map of FA_{PSDT} is the same as the map of FA which was shown in Figure 5. As we can see from Figures 5, 6, and 7, the map of GA is sharper than the map of FA_{PSDT}, while the latter can show more details. Comparing the map of FA_{PSDT} in Figure 7 with that in Figure 6, we can see that higher order tensors could improve the estimation of anisotropic diffusion as shown in Figure 7. In a word, these results show that the PSDT model can depict the characterization of diffusion anisotropy which is consistent with known neuroanatomy.

6. Conclusion. This paper proposed a novel model to estimate the ADC profiles by a positive semidefinite diffusion tensor (PSDT), which could be a second or higher order tensor. Features of this model include minimizing a convex optimization problem with a convex quadratic objective function constrained by the nonnegativity requirement on the smallest Z-eigenvalue of the diffusivity function. We also presented some numerical examples to illustrate the robustness and effectiveness of the PSDT model in the estimation of ADC profiles on synthetic data as well as MRI data. Experiment results show that higher order tensors could improve the estimation of anisotropic diffusion and that the PSDT model can depict the characterization of diffusion anisotropy which is consistent with known neuroanatomy.

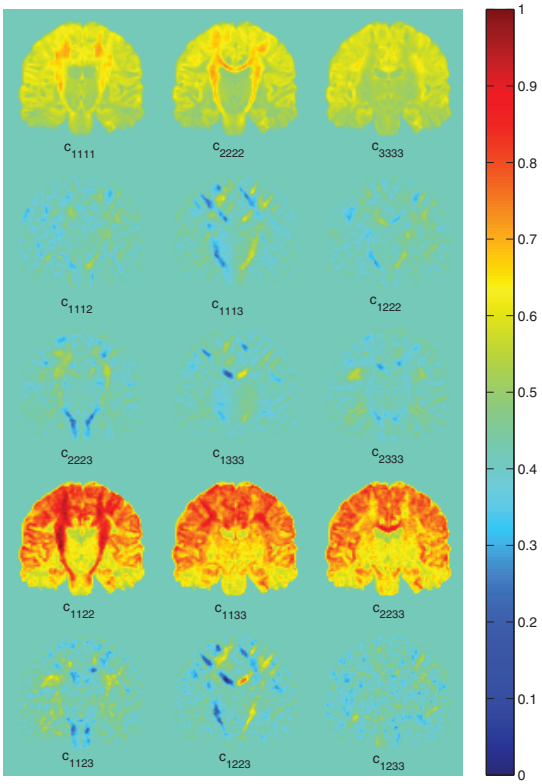

Figure 3. *Maps of coefficients of the ADC profile.*

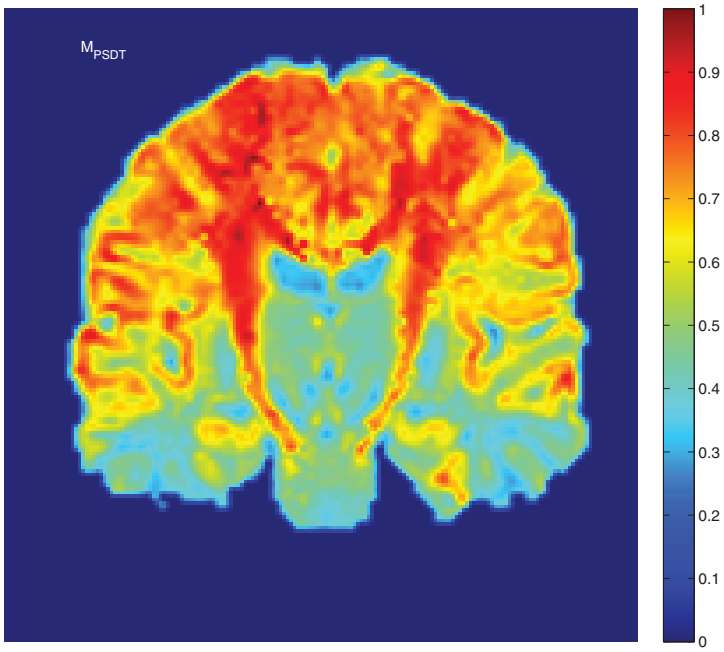

Figure 4. *The map of* M_{PSDT}.

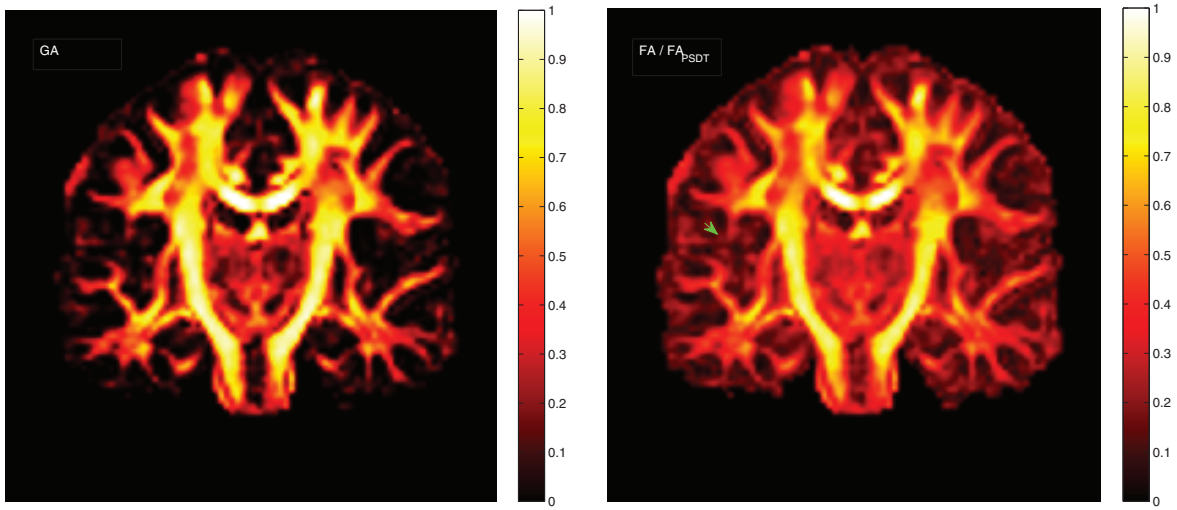

Figure 5. *Comparison of GA and FA_{PSDT}, fitting with a second order tensor.*

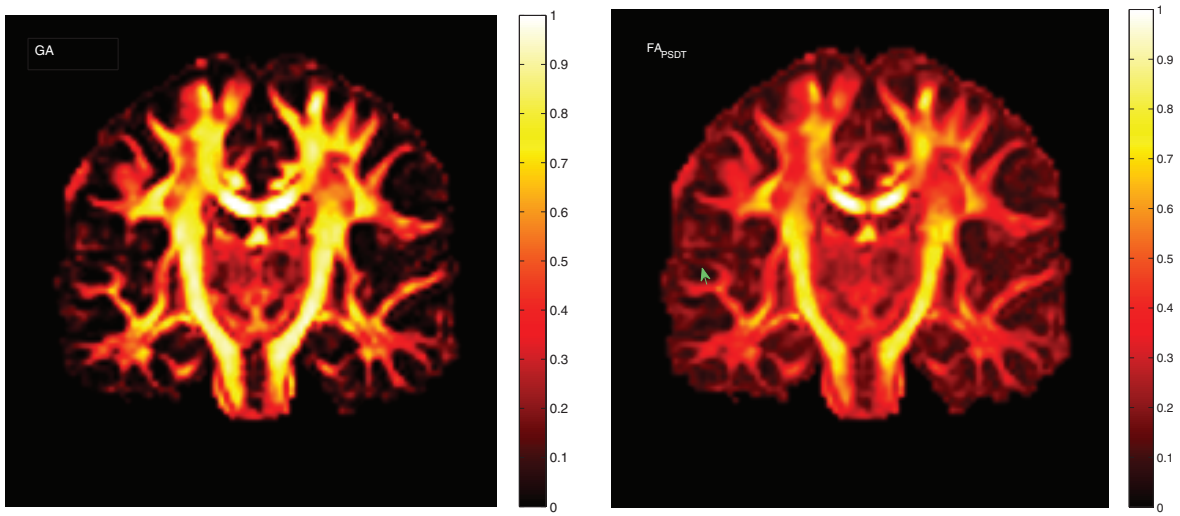

Figure 6. *Comparison of GA and FA_{PSDT}, fitting with a fourth order tensor.*

7. Appendix. The smallest Z-eigenvalue of a diffusivity function. To formulate an explicit constraint for (2.4), we need to have a measure for the extent of positive definiteness of a diffusivity function d. As d can be regarded as an mth order symmetric tensor, its smallest Z-eigenvalue introduced in [26] is a good measure for this purpose. The computational methods developed in [29] show that this measure is computable. See also [30, 28, 8]. We now describe such a method. Here we use the expression (2.1) to describe the method but actually use the Z-eigenvalue theory in [26, 29].

In fact, d is positive semidefinite if and only if the optimal value of the minimization

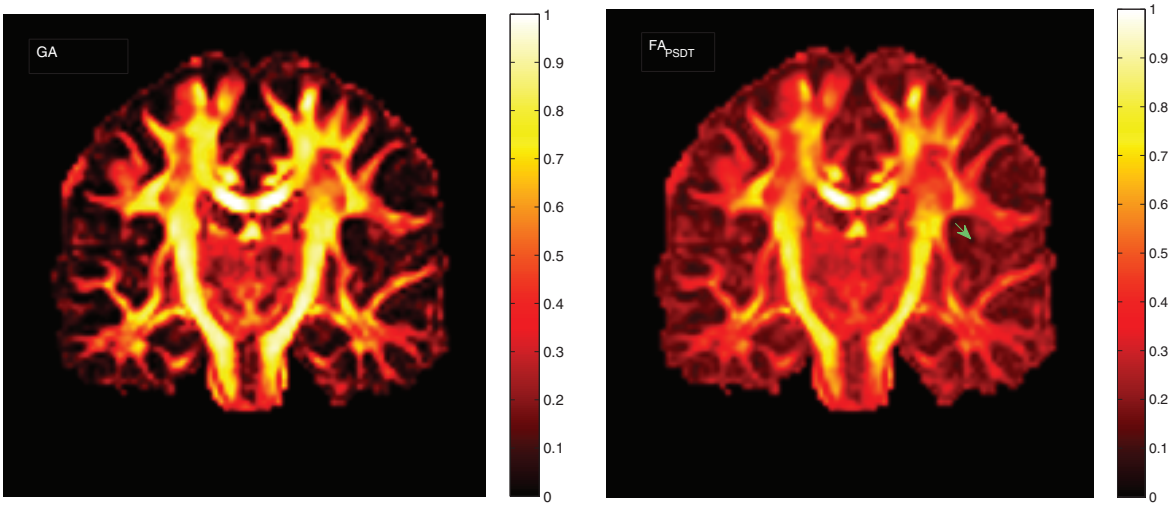

Figure 7. *Comparison of GA and FA_{PSDT}, fitting with a sixth order tensor.*

problem

$$\min\{d(\mathbf{g}) : g_1^2 + g_2^2 + g_3^2 = 1\} \tag{7.1}$$

is nonnegative. Problem (7.1) is not convex. Hence, we cannot use any local optimization method to solve it. As it has only three variables, we can find all of its stationary points and solve it. According to optimization theory, the optimality condition of (7.1) has the form

$$\begin{cases} \displaystyle\sum_{i=1}^{m}\sum_{j=0}^{m-i} i d_{ij} g_1^{i-1} g_2^j g_3^{m-i-j} &= m\lambda g_1, \\ \displaystyle\sum_{i=0}^{m}\sum_{j=1}^{m-i} j d_{ij} g_1^{i} g_2^{j-1} g_3^{m-i-j} &= m\lambda g_2, \\ \displaystyle\sum_{i=0}^{m}\sum_{j=0}^{m-i-1} (m-i-j) d_{ij} g_1^{i} g_2^{j} g_3^{m-i-j-1} &= m\lambda g_3, \\ g_1^2 + g_2^2 + g_3^2 &= 1. \end{cases} \tag{7.2}$$

The additional "m" on the right-hand side of each of the first three equations makes this optimality condition the same as the definition of Z-eigenvalues [26, 29, 8] for the symmetric tensor d. If $(\mathbf{g}, \lambda)$ is a solution of (7.2), then $\mathbf{g}$ is a stationary point of (7.1) and

$$\lambda = d(\mathbf{g}) \tag{7.3}$$

is a Z-eigenvalue of d. Then, the smallest Z-eigenvalue of d is the optimal value of (7.1).

We may solve (7.2) in the following way.

Case 1. $g_3 = g_2 = 0$. By (7.2), this happens only if $d_{m-1,1} = d_{m-1,0} = 0$. In this case, $g_1 = \pm 1$, $\lambda = d_{m,0}$.

Case 2. $g_3 = g_1 = 0$. By (7.2), this happens only if $d_{1,m-1} = d_{0,m-1} = 0$. In this case, $g_2 = \pm 1$, $\lambda = d_{0,m}$.

Case 3. $g_3 = 0$, $g_1 \neq 0$, and $g_2 \neq 0$. Then (7.2) becomes

$$\left\{\begin{array}{lcl} \sum_{i=1}^{m} i d_{i,m-i} g_1^{i-1} g_2^{m-i} & = & m\lambda g_1, \\ \sum_{i=0}^{m-1} (m-i) d_{i,m-i} g_1^{i} g_2^{m-i-1} & = & m\lambda g_2, \\ \sum_{i=0}^{m-1} d_{i,m-i-1} g_1^{i} g_2^{m-i-1} & = & 0, \\ g_1^2 + g_2^2 & = & 1. \end{array}\right. \tag{7.4}$$

We may eliminate λ in (7.4) and have the following equations of g_1 and g_2:

$$\left\{\begin{array}{lcl} \sum_{i=1}^{m} i d_{i,m-i} g_1^{i-1} g_2^{m-i+1} & = & \sum_{i=0}^{m-1} (m-i) d_{i,m-i} g_1^{i+1} g_2^{m-i-1}, \\ \sum_{i=0}^{m-1} d_{i,m-i-1} g_1^{i} g_2^{m-i-1} & = & 0, \\ g_1^2 + g_2^2 & = & 1. \end{array}\right.$$

Let $t = g_1/g_2$. We have

$$\left\{\begin{array}{lcl} \sum_{i=1}^{m} i d_{i,m-i} t^{i-1} & = & \sum_{i=0}^{m-1} (m-i) d_{i,m-i} t^{i+1}, \\ \sum_{i=0}^{m-1} d_{i,m-i-1} t^{i} & = & 0. \end{array}\right. \tag{7.5}$$

We may solve the two one-variable equations of (7.5) separately. If they have common solutions t, then (7.2) has solutions

$$g_1 = \frac{t}{\sqrt{1+t^2}}, \qquad g_2 = \frac{\pm 1}{\sqrt{1+t^2}}, \qquad g_3 = 0, \qquad \lambda = d(\mathbf{g}).$$

Case 4. $g_3 \neq 0$. We may eliminate λ in (7.2) and have the following equations of $\mathbf{g}$:

$$\left\{\begin{array}{lcl} \sum_{i=1}^{m} \sum_{j=0}^{m-i} i d_{ij} g_1^{i-1} g_2^{j} g_3^{m-i-j+1} & = & \sum_{i=0}^{m} \sum_{j=0}^{m-i-1} (m-i-j) d_{ij} g_1^{i+1} g_2^{j} g_3^{m-i-j-1}, \\ \sum_{i=0}^{m} \sum_{j=1}^{m-i} j d_{ij} g_1^{i} g_2^{j-1} g_3^{m-i-j+1} & = & \sum_{i=0}^{m} \sum_{j=0}^{m-i-1} (m-i-j) d_{ij} g_1^{i} g_2^{j+1} g_3^{m-i-j-1}, \\ g_1^2 + g_2^2 + g_3^2 & = & 1. \end{array}\right. \tag{7.6}$$

Let $u = g_1/g_3$, $v = g_2/g_3$. Then we have

$$\left\{\begin{array}{rcl} \displaystyle\sum_{i=1}^{m}\sum_{j=0}^{m-i} i d_{ij} u^{i-1} v^j & = & \displaystyle\sum_{i=0}^{m}\sum_{j=0}^{m-i-1} (m-i-j) d_{ij} u^{i+1} v^j, \\ \displaystyle\sum_{i=0}^{m}\sum_{j=1}^{m-i} j d_{ij} u^i v^{j-1} & = & \displaystyle\sum_{i=0}^{m}\sum_{j=0}^{m-i-1} (m-i-j) d_{ij} u^i v^{j+1}. \end{array}\right. \tag{7.7}$$

For solving system (7.7), we first regard it as a system of polynomial equations of variable u and rewrite it as

$$\left\{\begin{array}{l} \gamma_0 u^m + \gamma_1 u^{m-1} + \cdots + \gamma_m = 0, \\ \tau_0 u^{m-1} + \tau_1 u^{m-2} + \cdots + \tau_{m-1} = 0, \end{array}\right.$$

where $\gamma_0, \ldots, \gamma_m$, $\tau_0, \ldots, \tau_{m-1}$ are polynomials of v, which can be calculated by (7.7). By the Sylvester theorem, the above system of polynomial equations in u possesses solutions if and only if its resultant vanishes [10]. The resultant of this system of polynomial equations is the determinant of the $(2m-1) \times (2m-1)$ matrix

$$V := \begin{pmatrix} \gamma_0 & \gamma_1 & \cdots & \gamma_{m-2} & \gamma_{m-1} & \gamma_m & \cdots & 0 & 0 \\ 0 & \gamma_0 & \cdots & \gamma_{m-3} & \gamma_{m-2} & \gamma_{m-1} & \cdots & 0 & 0 \\ \cdot & \cdot & \cdots & \cdot & \cdot & \cdot & \cdots & \cdot & \cdot \\ 0 & 0 & \cdots & \gamma_1 & \gamma_2 & \gamma_3 & \cdots & \gamma_m & 0 \\ 0 & 0 & \cdots & \gamma_0 & \gamma_1 & \gamma_2 & \cdots & \gamma_{m-1} & \gamma_m \\ \tau_0 & \tau_1 & \cdots & \tau_{m-2} & \tau_{m-1} & 0 & \cdots & 0 & 0 \\ 0 & \tau_0 & \cdots & \tau_{m-3} & \tau_{m-2} & \tau_{m-1} & \cdots & 0 & 0 \\ \cdot & \cdot & \cdots & \cdot & \cdot & \cdot & \cdots & \cdot & \cdot \\ 0 & 0 & \cdots & \tau_0 & \tau_1 & \tau_2 & \cdots & \tau_{m-1} & 0 \\ 0 & 0 & \cdots & 0 & \tau_0 & \tau_1 & \cdots & \tau_{m-2} & \tau_{m-1} \end{pmatrix},$$

which is a polynomial equation in variable v. After finding all real roots of this polynomial, we can substitute them in (7.7) to find all the real solutions of u. Then, using

$$g_1 = \frac{u}{\sqrt{1+u^2+v^2}}, \qquad g_2 = \frac{v}{\sqrt{1+u^2+v^2}}, \qquad g_3 = \frac{\pm 1}{\sqrt{1+u^2+v^2}}, \qquad \lambda = d(\mathbf{g}),$$

we may find all the solutions of (7.2) in this case.

Combine all the possible solutions of (7.2) in these four cases, and find $\lambda_{\min}(d)$, the smallest value of λ of these solutions. Then $d \in \mathcal{S}$ if and only if $\lambda_{\min}(d) \geq 0$. This shows that the smallest Z-eigenvalue of d, i.e., $\lambda_{\min}(d)$, is computable. By [21], in the regular case, the number ν of Z-eigenvalues of d satisfies $\nu \leq m^2 - m + 1$. This implies that the degree of the one-dimensional polynomial equation in variable v is no more than $m^2 - m + 1$. This also implies that the complexity of finding $\lambda_{\min}(d)$ is in polynomial time.

Acknowledgments. The authors would like to thank Prof. Rachid Deriche and three anonymous referees for their comments and suggestions on the first version of this article, which led to significant improvements in the presentation.

REFERENCES

[1] D. C. Alexander, G. J. Barker, and S. R. Arridge, *Detection and modeling of non-Gaussian apparent diffusion coefficient profiles in human brain data*, Magn. Reson. Med., 48 (2002), pp. 331–340.

[2] V. Arsigny, P. Fillard, X. Pennec, and N. Ayache, *Log-Euclidean metrics for fast and simple calculus on diffusion tensors*, Magn. Reson. Med., 56 (2006), pp. 411–421.

[3] A. Barmpoutis, M. S. Hwang, D. Howland, J. R. Forder, and B. C. Vemuri, *Regularized positive-definite fourth order tensor field estimation from DW-MRI*, Neuroimage, 45 (2009), pp. S153–S162.

[4] A. Barmpoutis, B. Jian, B. C. Vemuri, and T. M. Shepherd, *Symmetric positive 4th order tensors & their estimation from diffusion weighted MRI*, in Information Processing in Medical Imaging, M. Karssemeijer and B. Lelieveldt, eds., Springer-Verlag, Berlin, 2007, pp. 308–319.

[5] P. J. Basser and D. K. Jones, *Diffusion-tensor MRI: Theory, experimental design and data analysis - a technical review*, NMR Biomed., 15 (2002), pp. 456–467.

[6] P. J. Basser, J. Mattiello, and D. LeBihan, *Estimation of the effective self-diffusion tensor from the NMR spin echo*, J. Magn. Reson. B, 103 (1994), pp. 247–254.

[7] P. J. Basser, J. Mattiello, and D. LeBihan, *MR diffusion tensor spectroscopy and imaging*, Biophys. J., 66 (1994), pp. 259–267.

[8] L. Bloy and R. Verma, *On computing the underlying fiber directions from the diffusion orientation distribution function*, in Medical Image Computing and Computer-Assisted Intervention—MICCAI 2008, Part I, Lecture Notes in Comput. Sci. 5241, D. Metaxas, L. Axel, G. Fichtinger, and G. Székeley, eds., Springer-Verlag, Berlin, Heidelberg, 2008, pp. 1–8.

[9] C. Chefd'Hotel, D. Tschumperle, R. Deriche, and O. Faugeras, *Regularizing flows for constrained matrix-valued images*, J. Math. Imaging Vision, 20 (2004), pp. 147–162.

[10] D. Cox, J. Little, and D. O'Shea, *Using Algebraic Geometry*, Springer-Verlag, New York, 1998.

[11] M. Descoteaux, E. Angelino, S. Fitzgibbons, and R. Deriche, *Apparent diffusion coefficients from high angular diffusion imaging: Estimation and applications*, Magn. Reson. Med., 56 (2006), pp. 395–410.

[12] M. Descoteaux, E. Angelino, S. Fitzgibbons, and R. Deriche, *Regularized, fast, and analytical q-ball imaging*, Magn. Reson. Med., 58 (2007), pp. 497–510.

[13] M. Descoteaux, N. Wiest-Daesslé, S. Prima, C. Barillot, and R. Deriche, *Impact of Rician adapted non-local means filtering on HARDI*, in Medical Imaging and Computer-Assisted Intervention—MICCAI 2008, Part II, Lecture Notes in Comput. Sci. 5242, Springer-Verlag, Berlin, Heidelberg, 2008, pp. 122–130.

[14] L. R. Frank, *Characterization of anisotropy in high angular resolution diffusion weighted MRI*, Magn. Reson. Med., 47 (2002), pp. 1083–1099.

[15] A. Ghosh, M. Descoteaux, and R. Deriche, *Riemannian framework for estimating symmetric positive definite 4th order diffusion tensors*, in Medical Image Computing and Computer-Assisted Intervention—MICCAI 2008, Lecture Notes in Comput. Sci. 5241, D. Metaxas, L. Axel, G. Fichtinger, and G. Székeley, eds., Springer-Verlag, Berlin, Heidelberg, 2008, pp. 858–865.

[16] J. L. Goffin and J. P. Vial, *Convex nondifferentiable optimization: A survey focused on the analytical center cutting plane method*, Optim. Methods Softw., 17 (2002), pp. 805–867.

[17] J.-B. Hiriart-Urruty and C. Lemaréchal, *Convex Analysis and Minimization Algorithms*, Springer-Verlag, Berlin, 1993.

[18] B. Jian, B. C. Vemuri, E. Özarslan, P. R. Carney, and T. H. Mareci, *A novel tensor distribution model for the diffusion-weighted MR signal*, Neuroimage, 37 (2007), pp. 164–176.

[19] C. Lenglet, J. Campbell, M. Descoteaux, G. Haro, P. Savadjiev, D. Wassermann, A. Anwander, R. Deriche, G. Pike, G. Sapiro, K. Siddiqi, and P. Thompson, *Mathematical methods for diffusion MRI processing*, Neuroimage, 45 (2009), pp. 111–122.

[20] C. Lenglet, M. Rousson, R. Deriche, and O. Faugeras, *Statistics on the manifold of multivariate normal distributions: Theory and application to diffusion tensor MRI processing*, J. Math. Imaging Vision, 25 (2006), pp. 423–444.

[21] G. Ni, L. Qi, F. Wang, and Y. Wang, *The degree of the E-characteristic polynomial of an even order tensor*, J. Math. Anal. Appl., 329 (2007), pp. 1218–1229.

[22] J. Nocedal and S. J. Wright, *Numerical Optimization*, Springer-Verlag, New York, 1999.
[23] E. Özarslan and T. H. Mareci, *Generalized diffusion tensor imaging and analytical relationships between diffusion tensor imaging and high angular resolution diffusion imaging*, Magn. Reson. Med., 50 (2003), pp. 955–965.
[24] E. Özarslan, B. C. Vemuri, and T. H. Mareci, *Generalized scalar measures for diffusion MRI using trace, variance, and entropy*, Magn. Reson. Med., 53 (2005), pp. 866–876.
[25] X. Pennec, P. Fillard, and N. Ayache, *A Riemannian framework for tensor computing*, Int. J. Comput. Vision, 66 (2006), pp. 41–66.
[26] L. Qi, *Eigenvalues of a real supersymmetric tensor*, J. Symbolic Comput., 40 (2005), pp. 1302–1324.
[27] L. Qi, *Eigenvalues and invariants of tensors*, J. Math. Anal. Appl., 325 (2007), pp. 1363–1377.
[28] L. Qi, D. Han, and E. X. Wu, *Principal invariants and inherent parameters of diffusion kurtosis tensors*, J. Math. Anal. Appl., 349 (2009), pp. 165–180.
[29] L. Qi, F. Wang, and Y. Wang, *Z-eigenvalue methods for a global polynomial optimization problem*, Math. Program., 118 (2009), pp. 301–316.
[30] L. Qi, Y. Wang, and E. X. Wu, *D-eigenvalues of diffusion kurtosis tensors*, J. Comput. Appl. Math., 221 (2008), pp. 150–157.
[31] R. T. Rockafellar, *Convex Analysis*, Princeton University Press, Princeton, NJ, 1970.
[32] K. Seunarine, P. Cook, M. Hall, K. Embleton, G. Parker, and D. Alexander, *Exploiting peak anisotropy for tracking through complex structures*, in Proceedings of the IEEE 11th International Conference on Computer Vision (ICCV 2007), IEEE Computer Society, Washington, DC, 2007, pp. 1–8.
[33] D. S. Tuch, *Q-ball imaging*, Magn. Reson. Med., 52 (2004), pp. 1358–1372.
[34] D. S. Tuch, T. G. Reese, M. R. Wiegell, N. G. Makris, J. W. Belliveau, and V. J. Wedeen, *High angular resolution diffusion imaging reveals intravoxel white matter fiber heterogeneity*, Magn. Reson. Med., 48 (2002), pp. 454–459.
[35] Z. Wang, B. C. Vemuri, Y. Chen, and T. H. Mareci, *A constrained variational principle for direct estimation and smoothing of the diffusion tensor field from complex DWI*, IEEE Trans. Med. Imaging, 23 (2004), pp. 930–939.
[36] N. Wiest-Daesslé, S. Prima, P. Coupé, S. P. Morrissey, and C. Barillot, *Rician noise removal by non-local means filtering for low signal-to-noise ratio MRI: Application to DT-MRI*, in Medical Imaging and Computer-Assisted Intervention—MICCAI 2008, Part II, Lecture Notes in Comput. Sci. 5242, Springer-Verlag, Berlin, Heidelberg, 2008, pp. 171–179.